JOURNAL OF SOLID STATE CHEMISTRY 114, 242–248 (1995)

Electronic Properties of $SrMnO_{3-x}$

K. J. Lee and E. Iguchi[1]

Department of Mechanical Engineering and Materials Science, Faculty of Engineering, Yokohama National University, Tokiwadai, Hodogaya-Ku, Yokohama 240, Japan

Received October 25, 1993; in revised form May 2, 1994; accepted May 4, 1994

Hexagonal four-layered (4L) and perovskite-like $SrMnO_{3-x}$ were prepared from equilibrium states at 1200 ~ 1600°C by quenching in water. Reoxidized specimens were also made by heating hexagonal 4L $SrMnO_{3-x}$ in air at 900°C for 24 hr and perovskite-like ones at 300°C for 0.5 hr. Dielectric properties and dc conductivities of quenched and reoxidized specimens were measured as a function of temperature. There is a distinct difference in conductivity between hexagonal 4L and perovskite-like $SrMnO_{3-x}$. The conductivity of hexagonal 4L $SrMnO_{3-x}$ does not change very much even if it is reoxidized, while the conductivity of cubic perovskite $SrMnO_3$ transformed from perovskite-like $SrMnO_{3-x}$ by reoxidation increases remarkably from conductivity before reoxidation. Dielectric relaxation peaks appear in the loss tangent in quenched specimens, but disappear in reoxidized specimens. The dielectric constants are greatly increased by reoxidation. These results are discussed based on crystal structures of $SrMnO_{3-x}$.

INTRODUCTION

The ABO_3 compounds (A, alkaline earth; B, transition metal) are of particular interest because of their potentially useful magnetic and electronic properties. In the case of B = Mn or Cu, furthermore, these compounds kindle strong interest in connection with high T_c superconductivity. Though the characterization of equilibrium phases in these materials by X-ray diffraction studies was difficult because of the mixed-valence states of B ions in a given phase, Negas and Roth have succeeded in investigating details of crystal structures of $SrMnO_{3-x}$ (1). Their result shows that the basic hexagonal structure of this material in air becomes increasingly anion-deficient with increasing temperature above 1035°C, reaching the limiting composition $SrMnO_{2.89}$ near 1400°C. Unit cell dimensions increase and distortion to orthorhombic symmetry occurs as oxygen content decreases. Further reduction occurs above 1400°C, and a perovskite-like homogeneity range exists from $SrMnO_{2.74}$ to $SrMnO_{2.62}$. The anion-deficient perovskite-like phases can be rapidly oxidized at low temperatures (near 300°C) to yield a metastable cubic perovskite $SrMnO_3$.

Although the magnetic properties of solid solutions of $SrMnO_3$–$LaMnO_3$ and $SrMnO_3$–$CaMnO_3$ have been studied extensively (2, 3), very little is known about isolated $SrMnO_3$. Other physical properties of isolated $SrMnO_{3-x}$, such as conduction kinetics, dielectric properties, and so on, have not been investigated yet. This must be because phase equilibria in this material have not been characterized. The results reported by Negas and Roth (1) now enable us to investigate the correlation between physical properties and phase equilibria in $SrMnO_{3-x}$. From this point of view, this report presents the electronic conductivity and dielectric properties of $SrMnO_{3-x}$ as functions of temperature and discusses these results in relation to the crystal structures obtained by Negas and Roth (1).

EXPERIMENTAL PROCEDURE

The $SrMnO_{3-x}$ ceramic specimens were prepared by a solid-state synthesis technique (1). Powders of $SrCO_3$ and MnO_2 (Johnson Matthey, 4N grade) were used. Several pellets were equilibrated in air at each desired temperature (1200, 1300, 1400, 1500, or 1600°C) and then quenched in water. A phase with an orthorhombic distortion of hexagonal four-layered $SrMn^{3+}_{2x}Mn^{4+}_{1-2x}O_{3-x}$ is in equilibrium at 1200 and 1300°C, while that of the perovskite-like structure of $SrMn^{3+}_{2x}Mn^{4+}_{1-2x}O_{3-x}$ is stabilized at 1500 and 1600°C (1). At 1400°C, a phase transition is expected to occur. One of the pellets equilibrated at each temperature was crushed into a powder and reoxidized at 900°C for 24 hr (equilibrium temperature 1200, 1300, or 1400°C) and at 300°C for 0.5 hr (equilibrium temperature 1500 or 1600°C). The gravimetric measurements determine magnitudes for x in $SrMnO_{3-x}$ by reoxidation. Powder X-ray diffraction patterns correspond well to the data reported by Negas and Roth (1). The reoxidized pellets were also prepared under the heating conditions described above.

Specimens are numbered using terminology such as S − 12Q or S − 12R, where the number 12 denotes the equilibrium temperature before quenching, i.e., 1200°C,

[1] To whom correspondence should be addressed.

0022-4596/95 $6.00

and "Q" or "R" represents the sample "as quenched" or "as reoxidized." Flat surfaces of the pellets were coated with a 7 : 3 In–Ga alloy by a rubbing technique for the electrode. HP4274A and 4284A LCR meters were used to measure capacitance and impedance. These electrodes were also used for dc conductivity measurements; that is, a two-probe method was employed because some heating processes (100 ~ 200°C) are required for preparations of four-probes, and crystal structures (1) and electronic properties are very sensitive to sample treatments even at such low temperatures, which will be described later. A Keithley 619 Resistance Bridge and an Advantest TR6871 digital multimeter with a high-ohm unit TR68704 were used for dc conductivity measurements. A copper–constantan thermocouple precalibrated at 4.2, 77, and 273 K was employed for temperature measurements. The measurements were taken at 1-K increments.

EXPERIMENTAL RESULTS

Gravimetric measurements yield $SrMnO_{2.942}$, $SrMnO_{2.931}$, $SrMnO_{2.869}$, $SrMnO_{2.737}$, and $SrMnO_{2.672}$ for S − 12Q, S − 13Q, S − 14Q, S − 15Q, and S − 16Q, respectively. The magnitudes for "x" in $SrMnO_{3-x}$ determined in this way agree well with the results obtained by Negas and Roth (1).

Figure 1 demonstrates the dielectric behavior of S − 16Q. The dielectric constant (ε') increases with increasing temperature (broken lines), but appears to have a maximum at about 280 K. Concerning the magnetic properties

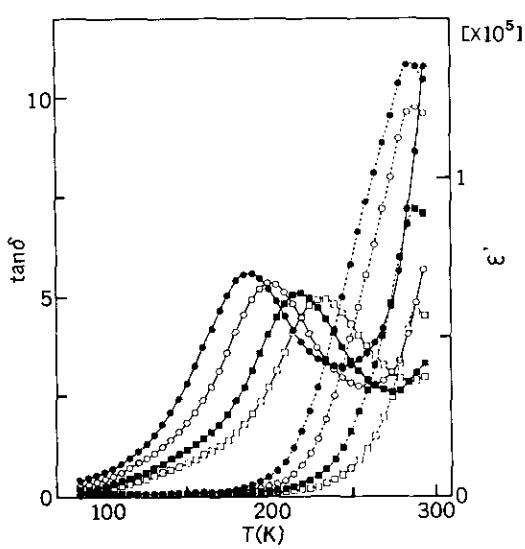

FIG. 1. Frequency dependence of the dielectric constants, ε' (broken lines), and the relaxation peaks in the loss tangent (solid lines) as a function of temperature. Solid circles represent the results at the applied frequency of 20 kHz; open circles, 40 kHz; solid squares, 100 kHz; and open squares, 200 kHz.

of cubic perovskite $SrMnO_3$, which transforms from an antiferromagnetic state to a paramagnetic state at 260 K (the Néel temperature) (4), it is very interesting to note that the temperature at which the dielectric constant has a maximum is close to the Néel temperature. A relaxation peak in the dielectric loss tangent is apparent in the temperature range 150–270 K. Debye's formula for tan δ is given by

$$\tan\delta \propto \frac{\omega\tau}{T(1+\omega^2\tau^2)}, \qquad [1]$$

where ω is the angular frequency, i.e., $2\pi f$, and τ is the relaxation time, which has the form $\tau_0 \exp(Q/k_B T)$, Q and k_B being the activation energy for the relaxation process and Boltzmann's constant, respectively. Then the resonant condition is

$$\omega\tau_0 \exp\left(\frac{Q}{k_B T_m}\right) = 1, \qquad [2]$$

where T_m is the temperature at which tan δ has a maximum value, which is represented by $(\tan\delta)_{max}$. As suggested by Debye's formula, Eq. [1], $(\tan\delta)_{max}$ decreases with increasing T_m, as shown in Fig. 1. Specimen S − 15Q shows quite similar dielectric behavior, but $(\tan\delta)_{max}$ is somewhat smaller in value than for S − 16Q (the ratio of $(\tan\delta)_{max}$ in S − 16Q to that in S − 15Q ≅ 1.4). As expected from Eq. [2], we have straight lines in the Arrhenius plots between applied frequencies (f) and $1/T_m$ with an activation energy of $Q = 0.194 \pm 0.004$ eV. After the reoxidation of S − 15Q and S − 16Q, the temperature dependence of the dielectric properties changes remarkably. The dielectric behavior of S − 15R at $f = 400$ kHz is illustrated as a function of temperature in Fig. 2. The magnitude of ε' increases after reoxidation. As temperature increases, the dielectric constant increases but one can recognize two obvious decreasing points, a small decrease at ~240 K and a considerably larger one at ~260 K. These temperatures are independent of the applied frequencies. The latter temperature is very close to the Néel temperature of cubic $SrMnO_3$, as well as of the specimens of S − 15Q and S − 16Q. Concerning the small decrease in ε' at ~260 K, we have no information. The dielectric relaxation observed in the loss tangents of quenched specimens disappears completely after reoxidation.

Specimens S − 12Q, S − 13Q, S − 14Q, S − 12R, S − 13R, and S − 14R exhibit behavior of the dielectric constant, ε', similar to that of S − 15Q and S − 16Q. In Fig. 3, we have plotted ε' of S − 12Q (the solid line) and S − 12R (the broken line) at $f = 10$ kHz. The magnitudes of ε' in the reoxidized specimens are large compared with those in the quenched ones, but the temperature depen-

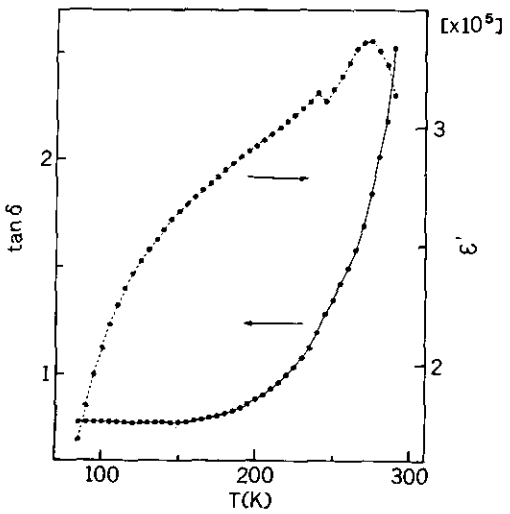

FIG. 2. The temperature dependence of the dielectric constant, ε' (the broken line), and the dielectric loss tangent, tan δ (the solid line), at the applied frequency of 400 kHz for specimen S − 15R.

dences are similar. Two dielectric relaxation peaks appear in the loss tangent in each of the quenched specimens S − 12Q, S − 13Q, and S − 14Q. Figure 4 demonstrates the realistic dielectric loss tangent of S − 12Q after subtraction of the background at $f = 10$ kHz. The peak height of these relaxations, $(\tan \delta)_{max}$, decreases as f increases. After reoxidation, they disappear completely, and the loss tangents increase smoothly with increasing temperature.

Arrhenius plots of σ and $1/T$ are given in Fig. 5. The conduction behavior of S − 15Q and S − 16Q is quite different from that of S − 12Q, S − 13Q, and S − 14Q,

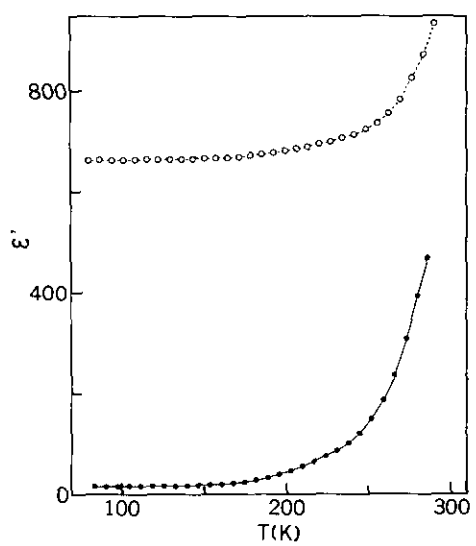

FIG. 3. The temperature dependences of the dielectric constant (ε') for specimens S − 12Q (solid circles) and S − 12R (open circles).

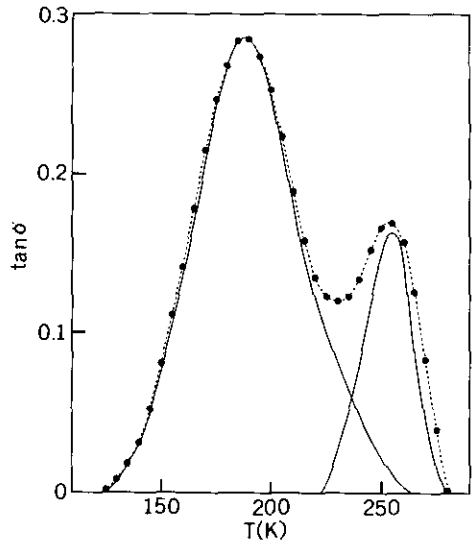

FIG. 4. The experimental values for realistic loss tangent (tan δ) versus temperature at $f = 10$ kHz after subtraction of background for specimen S − 12Q (solid circles and broken line). The solid lines are the theoretical curve calculated using Debye's equation with activation energy 0.18 eV for the low-temperature peak and 0.50 eV for the high-temperature peak.

as shown in Fig. 5a. The conductivity of S − 16Q is somewhat larger than that of S − 15Q (the ratio $\cong$ 1.4), but both specimens contain the same thermally activated processes of conduction in the entire temperature range measured. Below about 130 K, there are linear parts with an activation energy of 0.051 eV in the Arrhenius plots. Above 140 K, the conductivities seem to increase rather rapidly, but not in a linear form. After reoxidation, conductivities increase remarkably (S − 15R and S − 16R in Fig. 5b), and both these specimens have nearly the same conductivity. One can see the linear parts with an activation energy of 0.018 eV below about 140 K.

As for S − 12Q, S − 13Q, and S − 14Q (see Fig. 5a), conductivities are nearly independent of temperatures below ~140 K and they start to increase as temperature rises. It is likely that there are linear parts between $\log(\sigma)$ and $1/T$ with an activation energy of 0.525 ± 0.005 eV above ~230 K. These conductivities do not change drastically like those of S − 15R and S − 16R even if S − 12Q, S − 13Q, and S −14Q are heated at 900°C for 24 hr (see Fig. 5b). The conductivities of S − 12R and S − 13R increase slightly from those of S − 12Q and S − 13Q. The increment of conductivity in S − 14R from that of S − 14Q is larger if compared with those for S − 12R and S − 13R, but not by much.

DISCUSSION

A. *Perovskite-Like $SrMnO_{3-x}$ (S − 15Q and S − 16Q)*

In many oxides such as impurity-doped $BaTiO_3$, $Li_xNi_{1-x}O$, Li-doped α-Mn_3O_4, and WO_3, polarons are

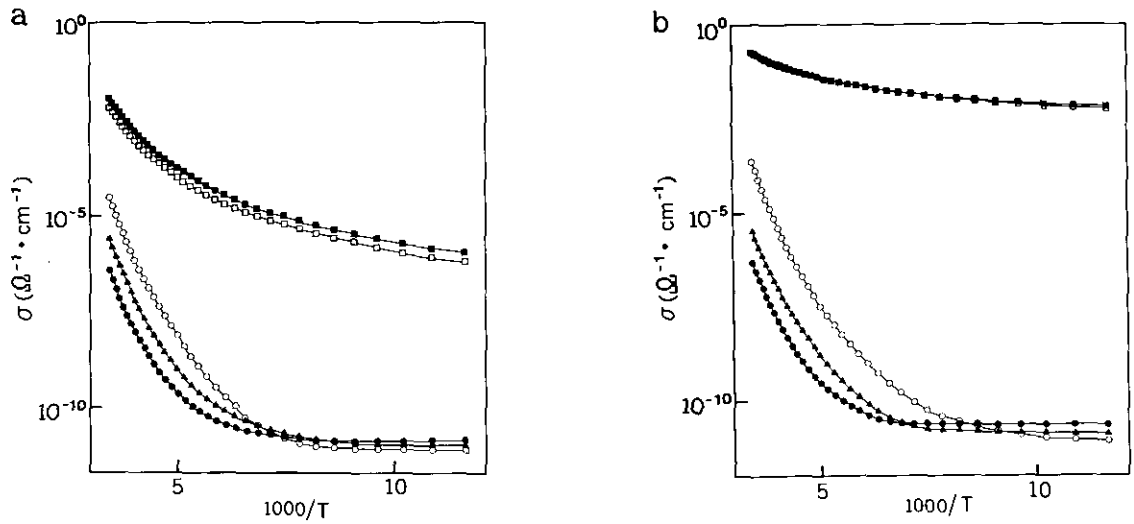

FIG. 5. The Arrhenius relations between σ and $1/T$ (a) for quenched specimens: solid circles, S − 12Q; solid triangles, S − 13Q; open circles, S − 14Q; open squares, S − 15Q; and solid squares, S − 16Q; (b) for reoxidized specimens: solid circles, S − 12R; solid triangles, S − 13R; open circles, S − 14R; open squares, S − 15R; and solid squares, S − 16R.

majority carriers and polaronic conductions take place (5–10). These oxides exhibit, in common, strong correlation between dielectric behavior and temperature dependence of conductivity; thermally activated process in the realistic loss tangent at the maximum, $(\tan \delta)_{max}$; and good agreement of the activation energy required for dielectric relaxation with that obtained in the Arrhenius plots between $\sigma \cdot T$ (or $\sigma \cdot T^{3/2}$) and $1/T$. Though dielectric relaxation is observed in quenched perovskite-like $SrMnO_{3-x}$ (S − 15Q and S − 16Q), it never shows thermally activated behaviors; that is, $(\tan \delta)_{max}$ decreases with increasing applied frequency, as indicated in Fig. 1. In addition, the activation energy for dielectric relaxation (0.194 eV) is quite different from that obtained from conductivity (0.051 eV). These results indicate no correlation between the relaxation observed in Fig. 1 and a polaron hopping process. An alternative possibility for this dielectric relaxation process is due to motions of Mn ions adjacent to oxygen vacancies. This is supported by the following experimental results. The ratio of x of S − 16Q to x of S − 15Q in $SrMnO_{3-x}$ is ~1.3, while the ratio of $(\tan \delta)_{max}$ of S − 16Q to that of S − 15Q and also the ratio of the conductivities of S − 16Q to those of S − 15Q is ~1.4. According to Negas and Roth (1), quenched specimens are represented by the formula $SrMn^{3+}_{2x}Mn^{4+}_{1-2x}O_{3-x}$ and Mn^{3+} ions are located at Mn sites adjacent to oxygen vacancies. Then, it is likely that the lattice distortions introduced by oxygen vacancies are sufficient to produce more than one potential minimum for Mn^{3+} ions, and the observed relaxation is associated with thermally activated motions between these minima under the action of alternating electric fields. Since the magnitude of $(\tan \delta)_{max}$ is proportional to the concentration of active dipole moments (i.e., Mn^{3+}) (11), the good agreement between the ratio of $(\tan \delta)_{max}$ and that of "x" in $SrMnO_{3-x}$ supports this conjecture.

The present results do not contain any experimental evidences supporting preferentially a polaronic conduction, as described before. Considering this fact, it seems that two alternative mechanisms are conceivable, instead of a polaronic conduction. First, we argue the band conduction of electrons. In such a case, the activation energy obtained in conductivities (i.e., ~0.051 eV) corresponds to the depth of the donor level from the bottom of the conduction band and the ratio of the conductivities in S − 16Q to those in S − 15Q (i.e., ~1.4) is theoretically equal to the ratio of the concentrations of conduction electrons which are thermally activated from donors. The ratio of the amount of Mn^{3+} in S − 16Q to that in S − 15Q (~1.3) leads to the conclusion that Mn^{3+} ions play an important role in conduction; i.e., the donor centers in quenched perovskite-like $SrMnO_{3-x}$ must be Mn^{3+} ions. The second possibility is as follows. For antiferromagnetic oxides, in general, there are electrons in the d band which interact with O^{2-} ions and they would be semiconductors if the crystal structures split the d band (12). The quenched perovskite-like $SrMnO_{3-x}$ involves electrons in the d band (i.e., Mn^{3+}) and the low point symmetry introduced by the oxygen deficiency has a high possibility to split the d band. However, such a conduction mechanism requires some overlap between Mn $3d$ wavefunctions and O $2p$ functions. Though the ratios for x in $SrMnO_{3-x}$, magnitude of $(\tan \delta)_{max}$, and conductivity between S − 15Q and S − 16Q can be explained self-consistently by

this mechanism, the rather large number of oxygen vacancies in quenched specimens prevent this mechanism from occurring in $SrMnO_{3-x}$ in practice. At the moment, then, band conduction looks more plausible but, unfortunately, there is no direct experimental evidence to show which mechanism is correct.

Above ~140 K, the conductivities of both specimens (S − 15Q and S − 16Q) increase, not in a linear form, as the reciprocal temperature decreases (Fig. 5a). Such behavior is in common to that in p-type NiO above ~90 K, which is ascribed to the antiferromagnetic effect (6, 13, 14).

B. Perovskite $SrMnO_3$ (S − 15R and S − 16R)

Quenched perovskite-like $SrMnO_{3-x}$ specimens are reoxidized very easily to cubic perovskite $SrMnO_3$. Even at 200°C, the dielectric relaxations observed in quenched specimens disappear. As the reoxidation progresses, the conductivities increase, and the results in Fig. 5b indicate that fully oxidized cubic perovskite specimens (S − 15R and S − 16R) have nearly the same conductivities in the entire temperature range measured, being independent of the equilibrium temperatures before quenching. Based upon analyses of XAS measurements on the $La_{1-x}Sr_xMnO_3$ series, Abbate *et al.* (15) conclude that the ground state of cubic perovskite $SrMnO_3$ is a mixture of $3d^3$ and $3d^4\,L$, where L denotes a ligand hole. This suggests that some overlap between the Mn $3d$ wavefunctions occurs through the oxygen ions in cubic $SrMnO_3$ as in other antiferromagnetic oxides (12). Then, one can expect conduction of electrons, perhaps through $3d^4\,L$ ligand holes, in the band which has weak interaction with O^{2-} ions and is therefore narrow. Such an interaction is possible, once most vacancies are occupied by O^{2-} ions in reoxidation. The activation energy required for the conduction in this narrow band must be 0.018 eV as obtained experimentally. As shown in Fig. 5b, carriers in cubic $SrMnO_3$ are very mobile and the polar effects of these mobile carriers under the action of alternating electric fields yield remarkable increases in dielectric constants of S − 15R and S − 16R as illustrated in Fig. 2.

C. Hexagonal 4L $SrMnO_{3-x}$

C.1. Surface layers in reoxidized specimens. As shown in Fig. 5, temperature dependencies of conductivities in quenched specimens (S − 12Q, S − 13Q, and S − 14Q) and reoxidized ones (S − 12R, S − 13R, and S −14R) are quite different from those of perovskite-like $SrMnO_{3-x}$ and cubic perovskite $SrMnO_3$. As demonstrated in Fig. 5b, the conductivities of specimens reoxidized at 900°C for 24 hr (S − 12R and S − 13R) are nearly equal to those of quenched ones, though slightly larger. As for S − 14R, conductivity increases from that of S − 14Q more obviously than occurs with S − 12R and S − 13R, but the temperature dependence of conductivities is similar to that of S − 14Q. These features do not change even if the heating time at 900°C is prolonged to 30 hr.

Though both the X-ray diffraction studies and the gravimetric measurements indicate that powders are completely reoxidized by heating at 900°C, there are practically no distinguishable changes in the results between quenched pellets and reoxidized pellets. Considering this fact, one can conjecture that it must be difficult to oxidize cores of pellets, perhaps because of low diffusion coefficients of oxygen in the hexagonal structure. Consequently, only thin layers just inside surfaces must be reoxidized. In order to confirm this, we have adopted two methods. One is to determine the mean valence of Mn ions in pellets by the chemical analysis employed by Nagashima *et al.* (16) and Mizutani *et al.* (17) and the other is to refer to the Maxwell–Wagner-type model, which is the simplest model of interfacial polarization in a capacitor with a double layer such as a material containing heterogeneous phases or absorption surface layers (18–20). Since the papers of Nagashima *et al.* (16) and Mizutani *et al.* (17) are written in Japanese, a framework for this chemical analysis is briefly introduced here. The powders crushed from pellets are mixed with 0.1 N $Na_2C_2O_4$. This is dissolved in 0.5N H_2SO_4 to reduce all the nominal Mn^{3+}/Mn^{4+} to Mn^{2+}. During this dissolution, the following reaction takes place:

$$Mn^{z+} + \frac{z-2}{2}(COO^-)_2 \rightarrow Mn^{2+} + (z-2)CO_2. \quad [3]$$

The amount of the unreacted $Na_2C_2O_4$ determined by the titration of $KMnO_4$ solution then yields the mean valences of Mn ions in pellets and, consequently, $3-x$ in $SrMnO_{3-x}$ can be determined. We prepared several specimens of S − 13Q and S − 13R with thickness 0.7 mm. Chemical analysis yields $SrMnO_{2.92}$ for S − 13Q, which is slightly less than the result determined by the gravimetric measurements, i.e., $SrMnO_{2.931}$, but still within the composition of the hexagonal structure (1). Next the surface layers with the thickness less than 0.1 mm are shaved from pellets of S − 13R and powders of the surface layers and the remaining cores are analyzed, respectively. Then, the average composition of the surface layers is $SrMnO_{2.98}$, while that of the cores is $SrMnO_{2.92}$, which is almost the same as the composition of S − 13Q. This result indicates that the surface layers are formed in the pellets of the hexagonal $SrMnO_{3-x}$ after reoxidation.

The Maxwell–Wagner model is, as known well, based upon a combination of two R–C parallel circuits; one represents the circuit of cores in pellets which have the quenched structure (i.e., not reoxidized) and the other the oxidized surface layers. The resultant admittance, Y,

is given by $Y = G + j\omega C$, where G and C denote the resultant conductance and capacitance, and ω is the applied angular frequency. In the Maxwell–Wagner model, then, the imaginary part of the ac conductivity is proportional to $\omega \cdot C$. Experimentally the imaginary part of ac conductivity is obtained by $1/|Z| \cdot \sin\theta$, where Z is the impedance and θ denotes the loss angle. Since the capacitance, C, is proportional to the dielectric constant, ε', one can expect, in a pellet reoxidized at 900°C, a linear relation between $1/|Z| \cdot \sin\theta$ obtained by impedance measurements and $\omega \cdot \varepsilon'$ obtained by capacitance measurements, while such a linear relation cannot be expected in quenched specimens. In Fig. 6, $\omega \cdot \varepsilon'$ of S − 13R and S − 13Q are plotted versus $1/|Z| \cdot \sin\theta$. We find a completely linear relation which is independent of both applied frequencies and temperatures for S − 13R. The quenched specimen, S − 13Q, has no linear relation. Nonlinear relations of S − 13Q obtained at several temperatures are also plotted in Fig. 6. Other specimens, S − 12Q, S − 14Q, S − 12R, and S − 14R, show quite similar behaviors. The results obtained by the chemical analysis and the dielectric behaviours based upon the Maxwell–Wagner-type model provide direct evidences that the surface layers are formed in reoxidized pellets of hexagonal 4L $SrMnO_{3-x}$.

As described before, a two-probe method was employed for dc conductivity measurements. Then, the resistance in the surface layer and that in the nonoxidized core are connected in series in so-called "reoxidized" specimens. Slight increases in the conductivity of S − 12R and S − 13R after reoxidation, as shown in Fig. 5, indicate the high conductivity of oxidized hexagonal 4L $SrMnO_3$, but very small volume fractions of surface layers contained in these specimens result in only slight increases in conductivities. According to Negas and Roth (1), at the equilibrium temperature, 1400°C, before quenching, the hexagonal 4L and perovskite-like $SrMnO_{3-x}$ coexist in equilibrium and their phase diagram (1) and x in $SrMnO_{3-x}$ yield 14% of perovskite-like $SrMnO_{3-x}$ in S − 14Q. As described above, perovskite-like $SrMnO_{3-x}$ is completely oxidized very rapidly to perovskite $SrMnO_3$ which has very high conductivity compared with quenched specimens (see Fig. 5b). When S − 14Q is heated at 900°C, perovskite-like $SrMnO_{3-x}$ is preferentially reoxidized. This leads to a rather large increment of conductivity in S − 14R from S − 14Q in comparison with S − 12R and S − 13R.

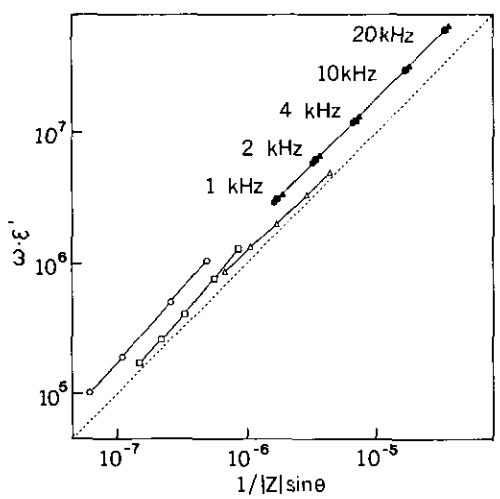

FIG. 6. The relation between $\omega \cdot \varepsilon'$ and $1/|Z| \cdot \sin\theta$ for specimens S − 13Q (open symbols) and S − 13R (solid symbols). Circles represent the plots obtained at 150 K under alternating electric fields with frequencies of 1, 2, 4, 10, and 20 kHz; solid squares, similar points obtained at 200 K; and solid triangles, at 250 K. All of the plots are on one line parallel to the broken line which represents the linear relation between $\omega \cdot \varepsilon'$ and $1/|Z| \cdot \sin\theta$. Each particular temperature has its own relation which is not parallel to the broken line.

C.2. Conductivities in quenched and reoxidized specimens. Though oxidized surface layers with low resistances result in increases in conductivities, nonoxidized $SrMnO_{3-x}$ cores with high resistances inside pellets rate-determine conductions of carriers because the resistances are connected in series. Consequently, thermally activated processes of conduction in so-called reoxidized specimens are quite similar to those in quenched specimens. In oxidized layers, carriers are more mobile than nonoxidized $SrMnO_{3-x}$ layers and the polar effects of these carriers yield increases in dielectric constants as shown in Fig. 3 as well as cubic perovskite $SrMnO_3$.

As shown in Fig. 4, S − 12Q, S − 13Q, and S − 14Q include two absorption peaks. The solid lines in Fig. 4 are the theoretical curve calculated using Debye's equation with activation energy 0.18 eV for the low-temperature peak and 0.50 eV for the high-temperature peak. According to Negas and Roth (1), there are two types of oxygen vacancy in quenched hexagonal $SrMnO_{3-x}$; one of them results in a Mn^{3+}–Mn^{4+} pair and the other leads to formation of a Mn^{3+}–Mn^{3+} pair. Referring to α-Mn_3O_4 (21, 22), these pairs are expected to make covalent bonds. Though the interpretation that two dielectric relaxations observed in quenched specimens correspond to motions of these pairs under the action of alternating fields looks very attractive, the conductivity results discourage this interpretation because these relaxation peaks disappear in reoxidized pellets in which most quenched structures of hexagonal $SrMnO_{3-x}$ are not yet reoxidized even if heated at 900°C for 24 hr. Thus we argue the following two possibilities. One is based upon the interpretation described above. In this case, the pairs Mn^{3+}–Mn^{4+} and Mn^{3+}–Mn^{3+} exist even after heating at 900°C, but this heating process removes the distortions introduced by quenching. The covalently bonded pair, then, must be

stabilized at a deep potential minimum and become unable to move under the actions of alternating fields. The other possibility is due to dielectric relaxations taking place in surface layers. In this case, however, we cannot identify relaxation mechanisms.

The activation energy required for conduction in S − 12Q, S − 13Q, and S − 14Q, 0.53 eV, is quite large in comparison with that of S − 15Q and S − 16Q. The 3*d* electrons which contribute to the formation of covalently bonded Mn^{3+}–Mn^{4+} and Mn^{3+}–Mn^{3+} pairs are also stabilized; that is, the covalent bonds result in deep trapping of 3*d* electrons in Mn ions. This leads to a wide energy gap between the donor level and the bottom of the conduction band in comparison with that in perovskite-like $SrMnO_{3-x}$. The activation energy obtained in conduction (0.53 eV) must correspond to this energy gap.

ACKNOWLEDGMENTS

The authors are very grateful to N. Kubota, W. H. Jung, and T. Masuda for assistance in this project and for useful discussion. This project was supported by a Grant-in-Aid for Science Research (No. 3650573) from the Ministry of Education, Science and Culture, Japan.

REFERENCES

1. T. Negas and R. S. Roth, *J. Solid State Chem.* **1,** 409 (1970).
2. G. H. Jonker and J. H. Van Santen, *Physica* **16,** 337 (1950).
3. J. B. MacChesney, H. J. Williams, J. F. Potter, and R. C. Sherwood, *Phys. Rev.* **164,** 779 (1967).
4. T. Takeda and S. Ohara, *J. Phys. Soc. Jpn.* **37,** 275 (1974).
5. E. Iguchi, N. Kubota, N. Nakamori, N. Yamamoto, and K. J. Lee, *Phys. Rev. B* **164,** 8646 (1991).
6. E. Iguchi and K. Akashi, *J. Phys. Soc. Jpn.* **61,** 3385 (1992).
7. E. Iguchi, K. J. Lee, and A. Iguchi, *J. Phys. Soc. Jpn.* **62,** 1135 (1993).
8. K. J. Lee and E. Iguchi, *J. Phys. Chem. Solids* **54,** 974 (1993).
9. E. Salje and G. Hoppman, *Philos. Mag. B* **43,** 105 (1981).
10. E. Iguchi, E. Salje, and R. J. D. Tilley, *J. Solid State Chem.* **38,** 342 (1981).
11. H. Fröhlich, *in* "Theory of Dielectrics," Chap. 3. Clarendon Press, Oxford, 1960.
12. I. G. Austin and N. F. Mott, *Adv. Phys.* **18,** 41 (1969).
13. Ya. M. Ksendoz, L. N. Ansel'm, L. L. Vasil'eva, and V. M. Latysheva, *Sov. Phys.—Solid State* **5,** 1116 (1963).
14. J. E. Keem, J. M. Honig, and L. L. Van Zandt, *Philos. Mag. B* **37,** 537 (1978).
15. M. Abbate, M. F. de Groot, J. C. Fuggel, A. Fujimori, O. Strebel, F. Lopez, M. Domke, G. Kaindl, M. Takano, Y. Takeda, H. Eisaki, and S. Uchida, *Phys. Rev. B* **46,** 4511 (1992).
16. K. Nagashima, M. Codell, and S. Fujiwara, *Bunseki Kagaku* **13,** 261 (1913). [In Japanese]
17. K. Mizutani, A. Kitazawa, N. Ookuma, and S. Katou, *Kougyou Kagaku Zasshi* **33,** 1097 (1992). [In Japanese]
18. K. W. Wagner, *Ann. Phys.* **40,** 817 (1913).
19. G. G. Koops, *Phys. Rev.* **83,** 121 (1951).
20. I. Bunnget and M. Popescu, *in* "Physics of Solid Dielectrics," Chap. 6. Elsevier, Amsterdam, 1984.
21. J. B. Goodenough and A. L. Loeb, *Phys. Rev.* **98,** 391 (1955).
22. K. Satomi, *J. Phys. Soc. Jpn.* **16,** 258 (1961).